

Towards combining prospective motion correction and distortion correction for EPI

R. Boegle¹, J. Maclaren¹, and M. Zaitsev¹

¹Dept. of Diagnostic Radiology, Medical Physics, University Hospital Freiburg, Freiburg, Baden-Württemberg, Germany

Introduction: In most fMRI studies, subject motion is assumed to be restricted to such a small amount that susceptibility-induced distortions can be treated as stationary and independent from motion. However, the ultimate goal of this project is to enable fMRI studies during significant head motion by applying prospective motion correction techniques [1]. In this regime, the motion dependence of susceptibility-induced distortions can no longer be neglected. The aim of this work is the correction of time-variant distortions in prospectively motion corrected echo planar images.

Theory and Methods: In this work, prospective motion correction using an external motion tracking device [1] is combined with both B_0 field inhomogeneity calculation using arbitrary magnetic susceptibility distributions [2], and geometric distortion correction [3]. This approach is demonstrated in a phantom study, using a specially designed phantom from earlier work [4], which is modelled as a susceptibility distribution. Additionally, field simulations based on a data set of a precisely segmented human head [5] are used to investigate the segmentation requirements necessary for applying this method *in vivo*, assuming that the susceptibility distribution of the subject's head would be obtained through a segmentation of structural MR images.

The method presented in [2], has already proven valuable for predicting field inhomogeneities, ΔB_0 , for a phantom in an arbitrary orientation with the B_0 field fixed in the z-direction [4]. However, for an object imaged during prospective motion correction, the B_0 field appears to rotate relative to the object, while the object appears to stay fixed in space. Therefore the apparent change in the B_0 field orientation has to be incorporated into the field calculation for the combined correction approach. This can be done by applying the Fourier rotation theorem. For an apparent rotation of the B_0 field around the x-axis of α° , the induced field in k-space is then,

$$\Delta \tilde{B}_0^{\tilde{z}}(\mathbf{k}, \alpha) = B_0 \left[\frac{1}{3} - \frac{(k_x \cos \alpha + k_y \sin \alpha)^2}{k_x^2 + k_y^2 + k_z^2} \right] \cdot \tilde{z}(\mathbf{k})$$

Inverse Fourier transformation yields the field inhomogeneities in image-space.

All experiments were performed on a Magnetom Trio 3T System (Siemens Healthcare, Germany). For empirical validation of the combined method, echo planar images and field maps were acquired using two sequences incorporating prospective motion correction: a spin echo EPI sequence (TR=2000 ms, TE=79 ms with an excitation angle of 90° and a refocusing pulse of 180°) and a double gradient echo sequence (TR=600 ms, TE1=9.84 ms, TE2=12.3 ms with an excitation angle of 25°). The sample-independent field inhomogeneities of the MR system were accounted for by shimming after acquiring a field map using a spherical oil phantom.

To illustrate the distortions that stem from rotation-induced changes in the field inhomogeneities, prospectively motion-corrected echo planar images of the custom-made phantom were acquired while it was rotated over an angular range of 60° . During the whole process the shim was fixed to a constant value. Additionally, field maps were acquired every 10° for comparison to the predicted field maps, as well as for comparative distortion correction using both predicted and acquired field maps.

The segmentation accuracy necessary for *in vivo* correction was investigated through field simulations, using susceptibility distributions derived from a publically available data set [5]. In the first simulation, the derived susceptibility distribution discriminated between white matter, gray matter, fat, blood, bone and air, with CSF and other tissues equal to water ('ground truth'). In the second simulation (the 'simple segmentation') this was reduced to bone and air, with all other tissues equal to water.

Results and Discussion:

Fig. 1 shows distortions in motion-corrected EPI of the phantom for two angles (A&B), as well as their correction with acquired (C&D) and calculated (E&F) field maps. The RMSE between all pairs of measured and calculated field maps is between 15-20 Hz, indicating good agreement between measurements and calculations. Thus, predicting the field maps using knowledge of object pose and susceptibility distribution is feasible. Fig. 2 compares the results of the field simulations based on the different segmentations. Good agreement is apparent (RMSE = 3.6 Hz for the whole brain), suggesting that a 'simple segmentation' is sufficient to estimate the most important B_0 field inhomogeneities. It would therefore be possible to apply this approach to distortion correction in prospectively motion-corrected EPI based fMRI. This would then allow correction even after large scale head motion, without the need to measure field maps for each head position in the time course.

Conclusion:

This proof-of-concept study shows that it is possible to correct for susceptibility-induced distortions in EPI after prospective motion correction, given a suitable susceptibility model of the imaged object. Simulations show that a simple segmentation (consisting only of tissue, bone and air) is sufficient.

Acknowledgements: This work is a part of the INUMAC project supported by the German Federal Ministry of Education and Research, grant #01EQ0605 and the "Real-time motion tracking and correction for MR and Spectroscopy" project supported by NIDA (IR01 DA021146).

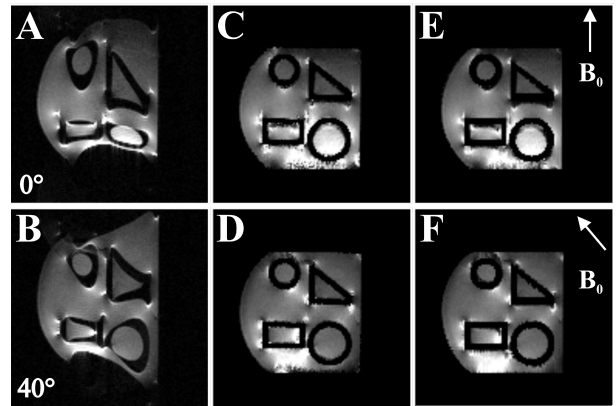


Fig. 1: prospectively motion corrected EPI with distortions still present (first column, A&B) and the correction of those with measured field maps (second column, C&D) and calculated field maps (third column, E&F) for different orientations of the phantom to B_0 , as indicated.

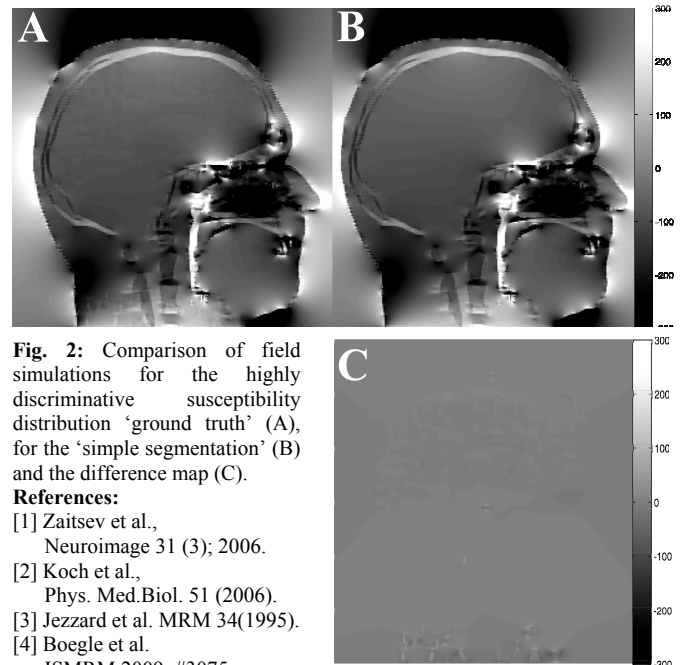


Fig. 2: Comparison of field simulations for the highly discriminative susceptibility distribution 'ground truth' (A), for the 'simple segmentation' (B) and the difference map (C).

References:

- [1] Zaitsev et al., Neuroimage 31 (3); 2006.
- [2] Koch et al., Phys. Med.Biol. 51 (2006).
- [3] Jezzard et al. MRM 34(1995).
- [4] Boegle et al. ISMRM 2009; #3075
- [5] http://www.itis.ethz.ch/index/index_humanmodels.html